# Coenzyme M biosynthesis in bacteria involves phosphate elimination by a functionally distinct member of the aspartase/fumarase superfamily

Received for publication, December 1, 2017, and in revised form, January 23, 2018 Published, Papers in Press, February 6, 2018, DOI 10.1074/jbc.RA117.001234

**Sarah E. Partovi[‡], Florence Mus[§], Andrew E. Gutknecht[‡], Hunter A. Martinez[‡], Brian P. Tripet[‡], Bernd Markus Lange[§¶], Jennifer L. DuBois[‡], and John W. Peters[§1]**

*From the [‡]Department of Chemistry and Biochemistry, Montana State University, Bozeman, Montana 59717 and the [§]Institute of Biological Chemistry and [¶]M. J. Murdock Metabolomics Laboratory, Washington State University, Pullman, Washington 99164*

Edited by Ruma Banerjee

**For nearly 30 years, coenzyme M (CoM) was assumed to be present solely in methanogenic archaea. In the late 1990s, CoM was reported to play a role in bacterial propene metabolism, but no biosynthetic pathway for CoM has yet been identified in bacteria. Here, using bioinformatics and proteomic approaches in the metabolically versatile bacterium *Xanthobacter autotrophicus* Py2, we identified four putative CoM biosynthetic enzymes encoded by the *xcbB1*, *C1*, *D1*, and *E1* genes. Only XcbB1 was homologous to a known CoM biosynthetic enzyme (ComA), indicating that CoM biosynthesis in bacteria involves enzymes different from those in archaea. We verified that the ComA homolog produces phosphosulfolactate from phosphoenolpyruvate (PEP), demonstrating that bacterial CoM biosynthesis is initiated similarly as the phosphoenolpyruvate-dependent methanogenic archaeal pathway. The bioinformatics analysis revealed that XcbC1 and D1 are members of the aspartase/fumarase superfamily (AFS) and that XcbE1 is a pyridoxal 5′-phosphate–containing enzyme with homology to D-cysteine desulfhydrases. Known AFS members catalyze β-elimination reactions of succinyl-containing substrates, yielding fumarate as the common unsaturated elimination product. Unexpectedly, we found that XcbC1 catalyzes β-elimination on phosphosulfolactate, yielding inorganic phosphate and a novel metabolite, sulfoacrylic acid. Phosphate-releasing β-elimination reactions are unprecedented among the AFS, indicating that XcbC1 is an unusual phosphatase. Direct demonstration of phosphosulfolactate synthase activity for XcbB1 and phosphate β-elimination activity for XcbC1 strengthened their hypothetical assignment to a CoM biosynthetic pathway and suggested functions also for XcbD1 and E1. Our results represent a critical first step toward elucidating the CoM pathway in bacteria.**

Coenzyme M (2-mercaptoethanesulfonate, CoM[2]) was once thought to be exclusive to methanogenesis in archaea, where it functions as a C1 carrier and plays a key role in the biosynthesis of methane gas (1–5). In the late 1990s, CoM was discovered to serve as a C3 carrier in a bacterial pathway for alkene metabolism in the proteobacterium *Xanthobacter autotrophicus* Py2 (6). Since then, other bacterial species from the Actinobacteria phylum have also been shown to use CoM in the metabolism of alkenes such as ethylene (6–11). In *X. autotrophicus* Py2, propylene is converted to acetoacetate, which is subsequently funneled into the tricarboxylic acid cycle in the form of two molecules of acetyl-CoA, where it serves as a carbon source for growth. The pathway begins with the epoxidation of propylene by an NADH-dependent alkene monooxygenase, forming propylene oxide. This is followed by nucleophilic attack by CoM to break the epoxide ring and form an enantiomeric mixture of *R*- and *S*-hydroxypropyl-CoM, catalyzed by epoxyalkane: CoM transferase (12–17). CoM then functions as a carrier, orienting *R*- and *S*-hydroxypropyl groups as oxidation substrates for a pair of stereoselective short-chain dehydrogenases, yielding 2-ketopropyl-CoM (16–18). In the final step of the pathway, CoM again serves to orient the 2-ketopropyl group for reductive cleavage and carboxylation, forming acetoacetate and free CoM (16, 17, 19–22). CoM, in essence, serves an analogous role in propylene metabolism as it does in methanogenesis, in promoting the proper orientation of these small organic substrates (16).

Methanogens have two known pathways for CoM synthesis, in which the carbon backbone for CoM is derived either from phosphoenolpyruvate (PEP) or L-phosphoserine (Scheme 1). The PEP-dependent pathway is initiated by a phosphosulfolactate synthase (ComA), which catalyzes the nucleophilic addition of sulfite to PEP (23, 24). The phosphosulfolactate product subsequently undergoes oxidative dephosphorylation to yield sulfopyruvate (25–28). Decarboxylation of sulfopyruvate, yielding sulfoacetaldehyde, is presumably followed by reduction and thiol addition to generate CoM (29, 30). The L-phosphoserine–

This material is based on work supported by the Department of Energy, Office of Science, Office of Basic Energy Sciences under Award Number DE-FG02-04ER15563. The authors declare that they have no conflicts of interest with the contents of this article.
This article contains Figs. S1–S5 and Table S1.

[1] To whom correspondence should be addressed: Institute of Biological Chemistry, Washington State University, 287 Clark Hall, 100 Dairy Rd., Pullman, WA 99164-1120. Tel.: 509-335-3412; Fax: 509-335-7643; E-mail: jw.peters@wsu.edu.

[2] The abbreviations used are: CoM, coenzyme M; PEP, phosphoenolpyruvate; AFS, aspartase/fumarase superfamily; PLP, pyridoxal phosphate; mBBr, monobromobimane; ppm, parts per million; Amp, ampicillin; Cm, chloramphenicol; PSL, phosphosulfolactate.

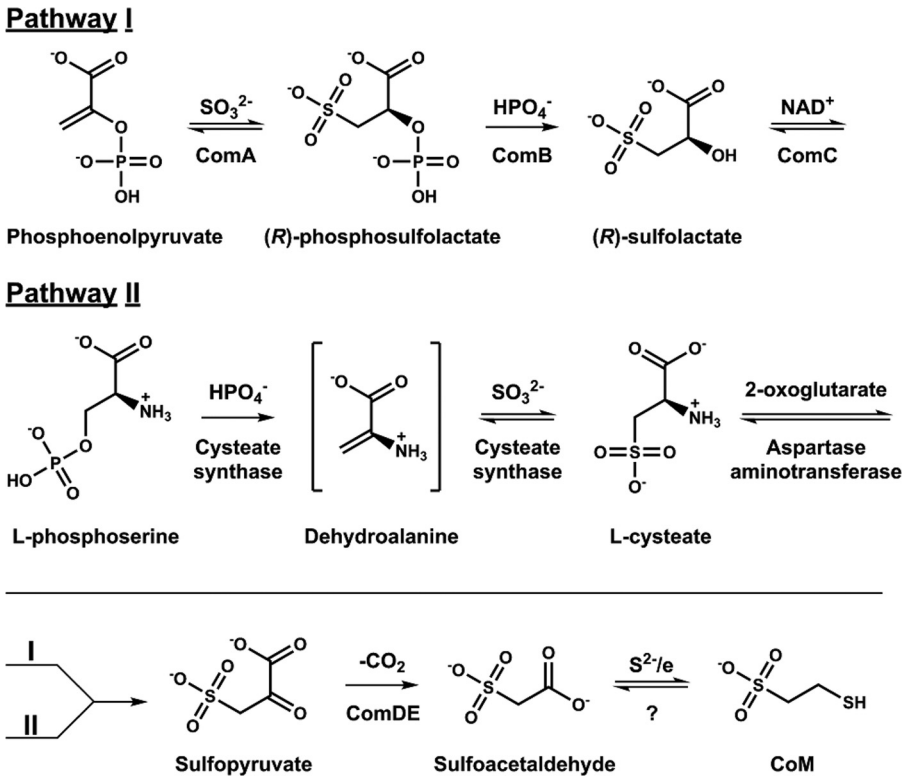


**Scheme 1. The PEP-dependent and L-phosphoserine–dependent pathways to CoM in methanoarchaea.** Pathway I and pathway II are depicted. Both pathways culminate in production of sulfopyruvate, which undergoes decarboxylation and reduction plus thiol addition to yield CoM.

dependent pathway begins with the concerted elimination of phosphate and addition of sulfite to generate L-cysteate. L-Cysteate is subsequently transaminated to form a common intermediate with the PEP dependent pathway, sulfopyruvate (31), and after that stage, the pathways are presumed to follow the same chemical steps as CoM.

Although it is essential for alkene metabolism, a bacterial pathway for CoM synthesis has never been described. The genes responsible for alkene metabolism in the bacterium *X. autotrophicus* Py2 are located on a 320-kb linear megaplasmid (pXAUT01) (Fig. 1) (32, 33). Proteomic experiments showed that proteins encoded in a gene cluster adjacent to the alkene-metabolizing genes were co-expressed with enzymes involved in propylene metabolism under conditions of propylene-dependent growth (14, 32). These experiments also revealed additional copies of the same genes. Only the cluster directly adjacent to the alkene-metabolizing genes is considered in this work, and these are designated *xcbB1*, *C1*, *D1*, and *E1* (XAUT_RS24680, RS24685, RS24690, and RS24695, respectively).

One of the genes in the cluster (*xcbB1*) is a homolog of *comA*, suggesting that the bacterial pathway for CoM biosynthesis is PEP-dependent. Additional genes within the cluster, however, are not similar to those from either methanoarchaeal pathways, suggesting that the bacterial CoM is synthesized via a chemically distinct series of reactions. The adjacent *xcbC1* gene encodes a member of the aspartase/fumarase superfamily (AFS). Enzyme families within this superfamily include the argininosuccinate lyases/δ2-crystallins, with which the XcbC1 gene product has the closest similarity, as well as class II fumarases, aspartases, and adenylosuccinate lyases. All of these AFS members catalyze β-elimination reactions that result in the formation of an unsaturated organic product (34).

In this work, we demonstrate that the ComA homolog XcbB1 catalyzes the conversion of PEP to phosphosulfolactate (Scheme 2). We also show that XcbC1 then catalyzes β-elimination using phosphosulfolactate as the substrate, releasing phosphate and sulfoacrylic acid as the analogous unsaturated product. This is a new activity for a member of the AFS and a highly unusual mechanism for biological dephosphorylation. Based on the confirmation of these two activities, bioinformatic analyses of the sequences for XcbD1 and E1, and partial biochemical characterization of XcbE1, we can now propose a complete biosynthetic pathway for CoM biosynthesis in bacteria.

## Results and discussion

### *Sequence analyses identify gene families and suggest possible roles for putative CoM biosynthetic genes*

The four putative CoM biosynthetic genes under study have deduced amino acid sequence similarities to characterized enzymes, providing clues regarding the likely chemical steps associated with bacterial CoM biosynthesis. The *xcbB1* gene is homologous to *comA*, which encodes the phosphosulfolactate synthase that initiates the PEP-dependent CoM biosynthetic pathway in methanogens. The pathway in *X. autotrophicus* Py2 is consequently presumed to be PEP-dependent. The adjacent *xcbC1* and *xcbD1* genes encode members of the AFS. Enzyme families within this superfamily catalyze reversible β-elimina-

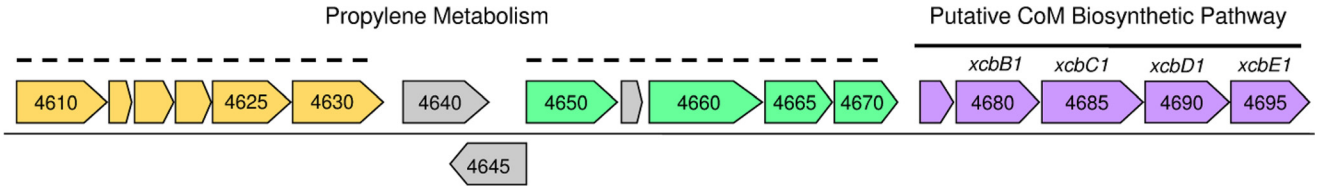


**Figure 1.** The 320-kb linear megaplasmid of *X. autotrophicus* Py2 contains the genes for the putative CoM biosynthetic pathway (*purple*) immediately downstream of the genes that encode the enzymes responsible for propylene metabolism. Alkene monooxygenase subunits are shown in *yellow*, and the remaining four enzymes involved in transforming propylene oxide to acetoacetate are shown in *green*. Alkene-related functions for the open reading frames shown in *gray* have not been assigned. The locus tags shown are truncated for clarity and contain the prefix "xaut_RS2" in the pXAUT01 plasmid.

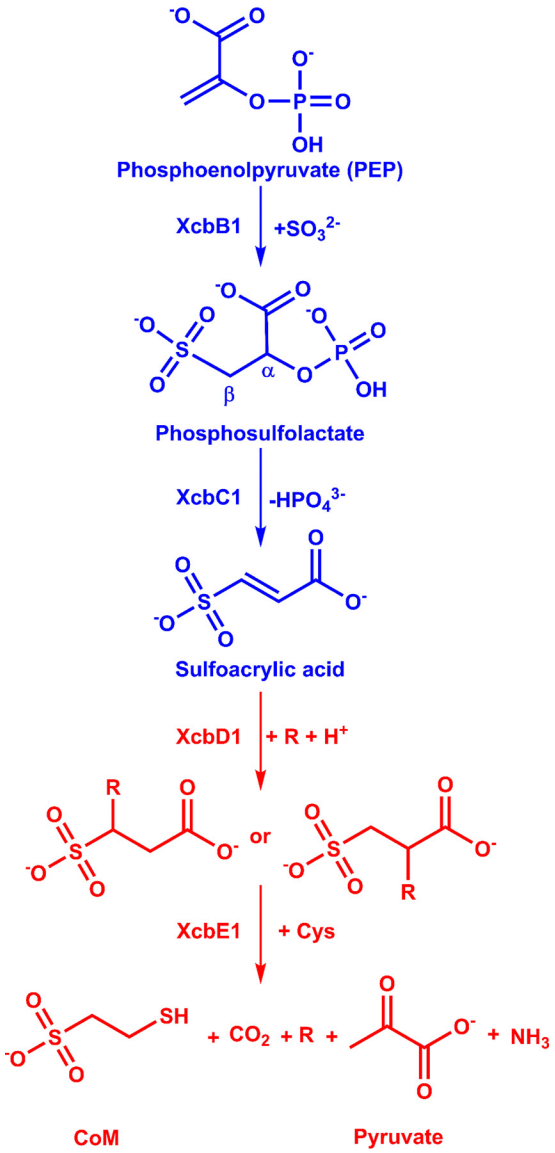


**Scheme 2. Proposed bacterial pathway for CoM biosynthesis.** Steps shown in *blue* are supported by data reported in this study. Steps shown in *red* are proposed based on bioinformatics analyses. Cysteine desulfhydrase activity has additionally been demonstrated for XcbE1 in the presence of either L- or D-Cys.

tion reactions that result in the formation of an unsaturated organic product (35–53). The last gene in the cluster, *xcbE1*, encodes a PLP-dependent enzyme homologous to D-cysteine desulfhydrases.

Using these preliminary sequence analyses, hypothetical roles for the enzymes in CoM biosynthesis have been proposed (Scheme 2). Homology between XcbB1 and ComA suggested that the pathway may begin with the addition of sulfite to PEP to form phosphosulfolactate. Conversion of this pathway intermediate to CoM requires net dephosphorylation, decarboxylation, and thiolation steps. The annotation of XcbC1 and XcbD1 as members of the AFS provides clear clues about the most logical trajectory by which these steps might occur. Within the AFS, XcbC1 has the strongest homology to the arginosuccinate lyases (Fig. 2). Enzymes in this family catalyze the reversible $\beta$-elimination of argininosuccinate through general base proton abstraction from the $C_\beta$ of the succinate moiety, yielding arginine and fumarate (35). Phosphosulfolactate is a loose structural analog of arginosuccinate, containing a potential proton abstraction site at the $C_\beta$ position relative to the phosphoryl group. A proton abstraction analogous to that catalyzed by argininosuccinate lyases would lead to elimination of phosphate and formation of a carbon– double bond, yielding sulfoacrylic acid. This product, in turn, is a structural analog of fumarate, the coproduct of the $\beta$-elimination of arginine.

The subsequent decarboxylation and thiolation steps are less clear, although the annotations are again enlightening of at least likely elements of the next steps. XcbD1 groups most closely with members of the adenylosuccinate lyase family within the AFS (Fig. 2), which catalyze the reversible elimination of AMP from adenylosuccinate to form fumarate (52). We propose that the most likely role for XcbD1 is therefore in catalyzing an analogous reaction in the addition direction, in which a substrate is added across the double bond. Attempts to use AMP as a substrate have not resulted in formation of adenylated product (data not shown). Addition of $H^+$ and an as yet undetermined co-substrate across the sulfoacrylic acid double bond (Scheme 2) would yield the putative substrate for XcbE1, the final enzyme in the pathway.

XcbE1 is homologous to pyridoxal phosphate (PLP)-dependent D-cysteine desulfhydrases that catalyze the $\alpha,\beta$-elimination of D-Cys to yield $H_2S$, pyruvate, and ammonia (54). We tested XcbE1 for desulfhydrase activity via $H_2S$ formation assays and found that both D- and L-Cys isomers were effective substrates, where XcbE1-specific activity was 27 ± 2 nmol $H^2S/min^{-1}$ mg-$XcbE1^{-1}$ for L-Cys and 5 ± 2 nmol $H_2S/min^{-1}$mg $XcbE1^{-1}$ for D-Cys (Fig. S1). It is attractive to propose, therefore, that XcbE1 supplies cysteine-derived sulfur that is ultimately incorporated into CoM. However, without knowing the product of the XcbD1 reaction, the cosubstrate for XcbE1 the mechanism of thiolation cannot yet be determined. In addition, the substrate of XbcE1 will also require decarboxylation to arrive at the CoM product. PLP-dependent enzymes catalyze a number of reactions, including decarboxylation, transamina-

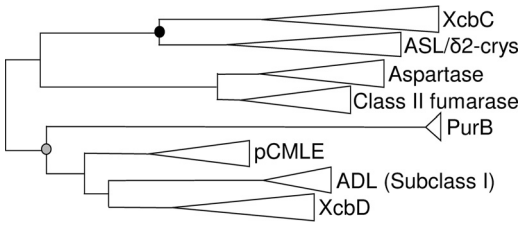


**Figure 2.** Bioinformatics analysis of XcbC1 (WP_011992986) and XcbD1 (WP_011992987) sequences identifies the AFS families to which each belongs is shown. The maximum likelihood tree (100 bootstrap reps) was constructed for XcbC1 and appears to show two subbranches for argininosuccinate lyase–type enzymes. Bootstrap values are shown only for nodes of relevance to this work, as indicated by *circles* (≥90, *black*; 80–89, *gray*). The canonical argininosuccinate lyase/δ2-crystallin enzymes appear to occupy a separate clade from the XcbC-type enzymes that may be involved in a pathway for CoM biosynthesis, and XcbD appears to form an additional subgroup in the adenylosuccinate lyase clade.

tion, racemization, and elimination/replacement reactions of a variety of predominantly amino acid substrates (55, 56). Many PLP-dependent enzyme reactions, moreover, share common intermediates, and several enzymes have been shown to be bifunctional, catalyzing combinations of reactions that utilize the basic PLP reaction chemistry (55). Examples include the decarboxylation and transamination catalyzed by dialkylglycine decarboxylase and the γ-elimination/β-replacement catalyzed by threonine synthase (57, 58). It is therefore conceivable that XcbE1 could be a bifunctional PLP enzyme, catalzying a more complicated final step coupling for example thiolation and decarboxylation in the production of CoM (Scheme 2).

### *XcbB1 catalyzes the conversion of phosphoenolpyruvate to phosphosulfolactate*

To begin to test these proposed steps of the pathway, we first examined the ComA homolog XcbB1. ComA catalyzes the addition of sulfite to PEP to yield phosphosulfolactate, an unusual metabolite that, according to currently annotated Kyoto Encyclopedia of Genes and Genomes (KEGG) pathway assignments, is unique to the methanogen PEP-dependent CoM biosynthetic pathway. An active site $Mg^{2+}$ in ComA coordinates the enol form of PEP, facilitating nucleophilic addition of sulfite and protonation of the adduct by a conserved active-site lysine to form phosphosulfolactate (24). The predicted phosphosulfolactate-producing activity of the ComA homolog XcbB1 was initially examined via sulfite consumption assays using monobromobimane (mBBr) as a fluorescent label for free sulfite (Fig. 3*A*). Sulfite consumption increased specifically when XcbB1 was incubated with the substrates PEP and sulfite, with a specific activity of 487 ± 45 nmol sulfite $min^{-1}$ $mg^{-1}$. This specific activity is ~20% of the activity reported for ComA from *Methanocaldococcus jannaschii*, supporting the conclusion that XcbB1 and ComA share the same physiological function (23). Q-TOF MS was subsequently used to identify phosphosulfolactate as the product (Fig. 3*B*). The predicted *m*/*z* for phosphosulfolactate in negative ion mode ((M-H)-species) was 248.94, which matched the *m*/*z* of the emergent signal in XcbB1-catalyzed reactions. Additionally, the isotope distribution matched the predicted isotope distributions within 5% of their predicted values.

Time-resolved $^1$H NMR directly demonstrated the consumption of PEP and concomitant production of phosphosulfolactate by XcbB1 in real time (Fig. 3*C*; see also Fig. S2 for $^1$H NMR spectra of pure standards). At pH 8, the pair of singlets associated with the PEP vinyl moiety (5.15 and 5.35 ppm) showed clear signs of consumption in the presence of bisulfite ($HSO_3^-$) and XcbB1 (Fig. S4*A*). PEP consumption was temporally coupled to phosphosulfolactate production, detected via the increase of a characteristic doublet signal (3.36/3.35 ppm) upfield. The phosphosulfolactate triplet signal was not visible, likely because of the suppression of the water peak, plus the additional Tris and glycerol peaks in the 3.5–4.8 ppm region. The reaction went to completion within 30 min, consistent with the general time course for sulfite consumption expected from the specific activity measured in Fig. 3. We therefore assign XcbB1 as a PEP-dependent phosphosulfolactate synthase (EC:4.4.1.19).

### *XcbC1 catalyzes the β-elimination of phosphate from phosphosulfolactate to form sulfoacrylic acid*

The proposed substrate for XcbC1 is the phosphosulfolactate generated by the upstream enzyme XcbB1. In keeping with its sequence-based assignment to the arginosuccinate lyase family, the proposed β-elimination to yield phosphate was monitored using a coupled assay involving XcbB1, XcbC1, and molybdenum blue as a phosphate indicator (Fig. 4*A*). When equimolar amounts of XcbB1 and XcbC1 were present in solution with a large excess of PEP and sulfite, a robust level of phosphate production was observed (specific activity = 30 ± 8 nmol $PO_4^{3-}$ $min^{-1}$ mg $XcbC1^{-1}$). We therefore concluded that XcbC1 catalyzes the dephosphorylation of phosphosulfolactate, which was in turn generated by the upstream catalyst XcbB1.

Canonical alkaline/acid phosphatases are typically metal-dependent enzymes that catalyze the hydrolysis of phosphomonoesters using metal-activated water, resulting in inorganic phosphate and alcohol products (59–65). A classic phosphohydrolase-type reaction would be expected to yield sulfolactate from phosphosulfolactate (Fig. S3*A*). However, Q-TOF MS analysis of the reaction products indicated that sulfoacrylic acid was the organic product (Fig. 4*B*), based on its measured *m*/*z* (150.967, (M-H)-species, negative ion mode) and isotope pattern. These matched predicted values for sulfoacrylic acid (*m*/*z* = 150.97) rather than sulfolactate (*m*/*z* = 168.98). This suggested that XcbC1 does not catalyze a simple hydrolytic reaction on the phosphosulfolactate substrate; rather, the reaction requires concomitant release of phosphate and a proton to form an unsaturated product, consistent with β-elimination (see below).

Time-resolved $^1$H NMR of the XcbC1 reaction directly demonstrated that disappearance of the doublet signal attributed to phosphosulfolactate was coupled with the appearance of a new pair of doublets further downfield (6.96/6.93 and 6.53/6.50 ppm, integrated to 1) (Fig. S4*B*). These doublets match the predicted $^1$H NMR spectrum for sulfoacrylic acid (Fig. 4*C* and Fig. S3*B*). The measured spectrum furthermore bears no overlap with the $^1$H NMR spectrum observed for a sulfolactate standard (Fig. S2*B*), confirming the production of a new double bond. The large j-values for the pair of doublets (16.08) indicate significant separation of the olefinic hydrogens relative to each

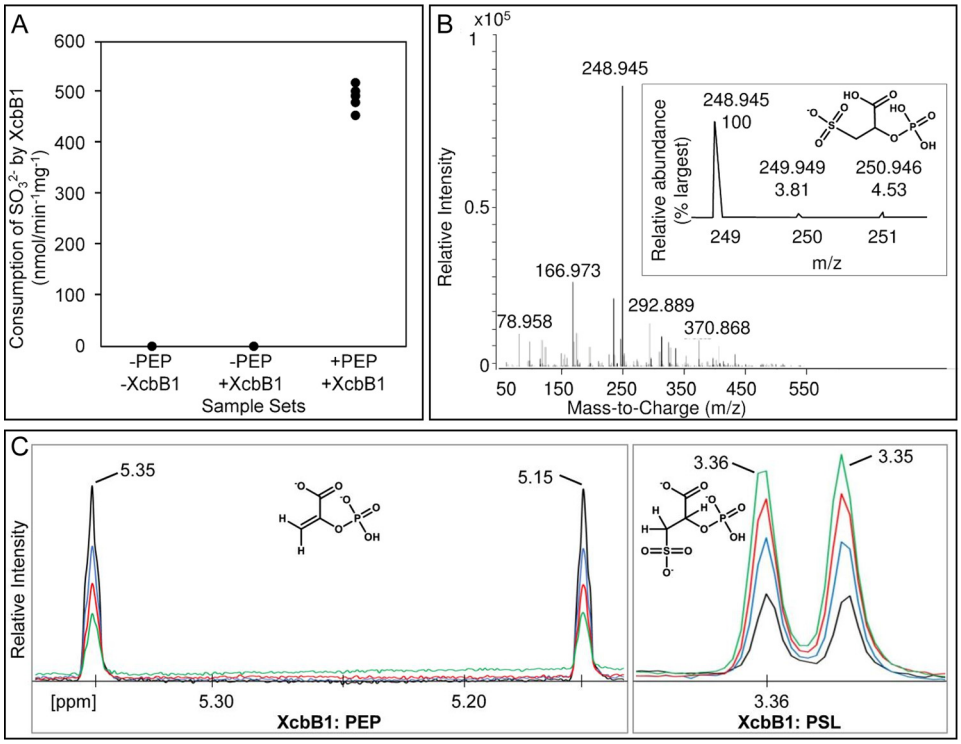


**Figure 3.** The XcbB1 reaction was established using biochemical and spectroscopic means. *A*, using fluorescence spectroscopy, the consumption of 1 mM sulfite by purified XcbB1 was measured with or without the presence of 1 mM PEP. An increase in sulfite consumption is observed specifically in samples containing PEP. *B*, MS analysis of the products of the XcbB1-catalyzed reaction demonstrate production of phosphosulfolactate from 5 mM PEP and 5 mM sulfite. The *inset* shows the isotope distribution of phosphosulfolactate along with the corresponding ratios. The predicted *m/z* 248.945 and the respective predicted isotope distribution agree with the findings. *C*, time-resolved $^1$H NMR spectroscopy of the XcbB1 reaction shows the consumption of 2 mM PEP with the addition of 1 mM sulfite on the *left*, with the concomitant yield of phosphosulfolactate (PSL) on the right. Spectra were monitored continuously over time. For clarity, four time points are shown (0–2 min, *black*; 8–10 min, *blue*; 16–18 min, *red*; 28–30 min, *green*). For all experiments, samples included 0.1 mg of XcbB1 in pH 8 buffer and were incubated at 30 °C.

other, meaning that the XcbC1 product exists specifically in the *trans* conformation. The conversion of phosphosulfolactate to sulfoacrylic acid proceeded to completion within ~12–14 min, again consistent with the reaction time scale indicated by the phosphate release data in Fig. 4*A*. We therefore conclude that XcbC1 is an unusual AFS-type phosphatase that catalyzes a $\beta$-elimination reaction using phosphosulfolactate as the substrate.

### *Modeling XcbC1 active site reactivity*

The sequence of XcbC1 was analyzed in light of canonical AFS structures and mechanisms to understand the features that permit its unique reactivity. AFS members share a signature GSS*XX*P*X*K*X*N sequence, tertiary/quaternary fold, and active site structure and a general acid-base catalytic strategy, even while their sequence identities may be comparatively low (20–30%) (Fig. S5) (40). Canonical AFS enzymes have been proposed to use a general base for proton abstraction from the C$\beta$ atom of the substrate, followed by collapse of the carbanion intermediate and cleavage of the substrate. Product release may be facilitated by donation of a proton from an active-site acid to the leaving group (34). Mutagenesis and structural studies point toward the strictly conserved first serine of the GSS*XX*-P*X*K*X*N motif as the base (35, 50, 66). Interactions with backbone amides or the $\beta$-carboxylate group of the substrate may stabilize the catalytic Ser in its oxyanion form (41, 48). The catalytic acid has been proposed to be an incompletely conserved histidine residue in argininosuccinate lyase/δ2-crystallin, adenylosuccinate lyases, and fumarate lyases, with various replacements in aspartases and members of the pCMLE (3-carboxy-*cis,cis*-muconate lactonizing enzyme) family (35, 40, 50). Finally, a strictly conserved lysine has been shown to interact with and position the $\alpha$-carboxylate group of the substrate (41, 66). The substrate-binding cavity otherwise appears to be variable, with various residues stabilizing substrates through an extensive hydrogen bonding network (50, 66).

A homology-modeled structure for XcbC1 was generated using the crystal structure for a closely related δ2-crystallin in its argininosuccinate-bound form (Fig. 5*A*) (40). Residues from the crystal structure that were proposed to interact with the substrate are superimposed with the corresponding residues from the XcbC1 homology model. XcbC1 appears to retain the catalytic base (Ser-285B, XcbC1 numbering) and strictly conserved lysine (Lys-291B) but very little else. Apart from the residues important for catalysis, the other residues highlighted for δ2-crystallin form a stabilizing hydrogen bonding network around argininosuccinate (40, 67). Notably, the catalytic His is absent in the XcbC1 model, with Tyr-164A–Ala-298B replacing His-162A–Glu-296B. Previous mutagenesis studies of aspartase from *Bacillus* sp. YM55-1 showed that the histidine is not absolutely required for activity and, when considered with the incomplete conservation of the residue, may indicate that the protonation of the substrate leaving group varies among the

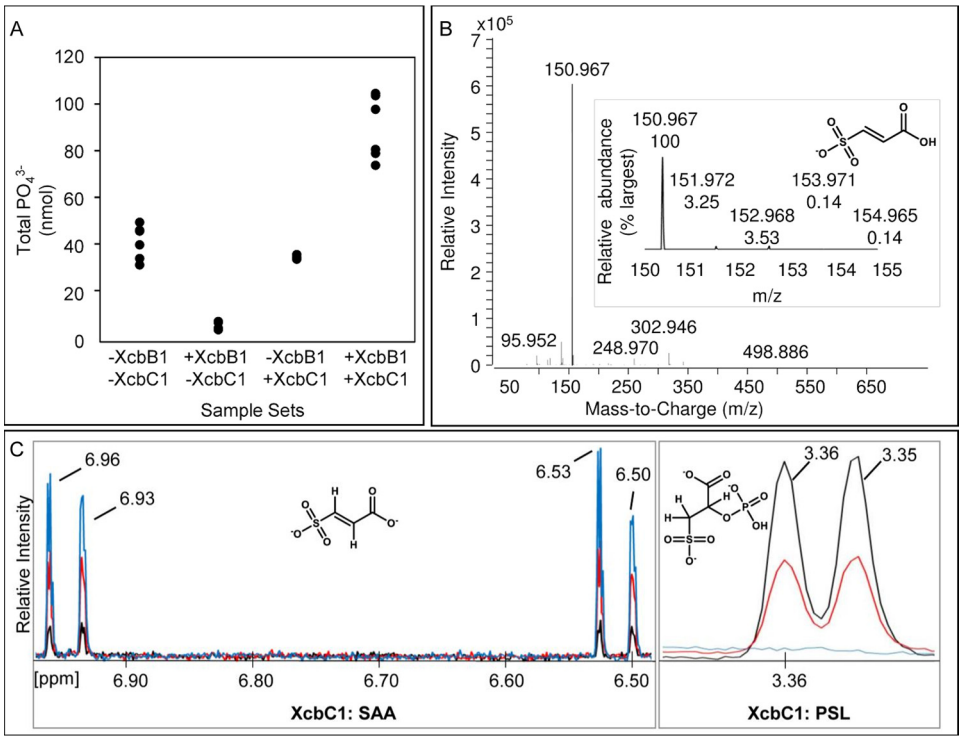


**Figure 4.** The XcbC1 reaction was established through biochemical and spectroscopic means. *A*, the production of phosphate was monitored from a coupled assay containing 1 mM PEP, 1 mM sulfite, and one, both, or neither enzyme (XcbB1 and XcbC1). Inorganic phosphate, measured via absorbance using the molybdenum blue assay, was produced only in the presence of both XcbB1 and C1, suggesting that the latter removes phosphate from the XcbB1 product, phosphosulfolactate. *B*, the products of the coupled assay initiated by 5 mM PEP and 5 mM sulfite were analyzed by MS. The *inset* shows the isotope distribution of sulfoacrylic acid along with the corresponding ratios. The predicted *m/z* 150.970 and the respective predicted isotope distribution are in agreement with the results. *C*, time-resolved $^1$H NMR showed conversion of PSL to sulfoacrylic acid (*SAA*) over time by the XcbB1/C1-coupled reaction, initiated by 2 mM PEP and 1 mM sulfite. For clarity, only three time points are shown (0–2 min, *black*; 8–10 min, *red*; 28–30 min, *blue*). XcbC1 appears to fully convert PSL before the 30 min end point. For all experiments, samples included 0.1 mg of XcbB1 in pH 8 buffer and were incubated at 30 °C.

superfamily (34, 43). Using the homology model and known AFS chemistry, it is possible to propose a catalytic mechanism for XcbC1 (Fig. 5*B*). Like the canonical AFS enzymes, the conserved Ser-285B could feasibly initiate the general base-catalyzed reaction through abstraction of the phosphosulfolactate C$\beta$ proton, which we expect to have a relatively high pKa, with stabilization from Lys-291B and putative H-bond donors present in the binding site. If the phosphoryl group of phosphosulfolactate is already singly protonated, it is possible that acid catalysis is not needed to facilitate phosphate release (phosphate pKa values = 2.12 and 7.21). Hence, it is plausible that, distinct from the proposed aspartase/fumarase mechanism (34), proton abstraction and phosphate release from phosphosulfolactate occur in a concerted step. Interestingly, a similar $\beta$-elimination resulting in the release of phosphate was recently described for the OspF family of bacterial enzymes (68, 69). These catalyze the removal of phosphate from phosphothreonine, generating dehydrobutyrine (an alkene) using a conserved Lys and His as a base and acid, respectively. This so-called "eliminylation" reaction bears intriguing similarities to the proposed reaction catalyzed by XcbC1, although the OspF family does not appear to be evolutionarily related to the aspartate/fumarate lyases, and XcbC1/OspF enzymes share little homology.

### *Conclusions*

Investigating the putative gene products of *xcbB1* and *xcbC1* by informatics, biochemical, and spectroscopic means provided a critical first step toward elucidating a PEP-dependent pathway for bacterial CoM biosynthesis that is distinct from the PEP-dependent pathway in methanogens. Of the four enzymes possibly involved in CoM biosynthesis, only XcbB1 is homologous to the pathway enzyme ComA, which is known to encode the first step in the PEP-dependent CoM biosynthesis in methanogens. XcbB1 catalyzes the addition of sulfite to PEP to yield phosphosulfolactate, which is delivered as the substrate for the subsequent XcbC1 reaction. The $\beta$-elimination of phosphate catalyzed by XcbC1 yields sulfoacrylic acid and inorganic phosphate. To our knowledge, this reaction has not been observed before in AFS enzymes, marking a novel activity for an enzyme from a large, well-characterized family as well as a novel pathway intermediate. Although the activity of XcbD1 remains unidentified, we have implicated an important hypothetical role for PLP-dependent XcbE1 in providing the source of the CoM thiol derived from Cys. This work will serve as the framework for future studies aimed at uncovering the final stages of the biosynthetic pathway. By elucidating the XcbB1 and XcbC1 reactions, we have made significant strides toward understanding bacterial CoM biosynthesis, which has evaded characterization in previous years.

## Experimental procedures

### *Growth of X. autotrophicus Py2*

Cells were grown as described previously in phosphate buffer, assorted nutrients, and trace minerals at 30 °C with

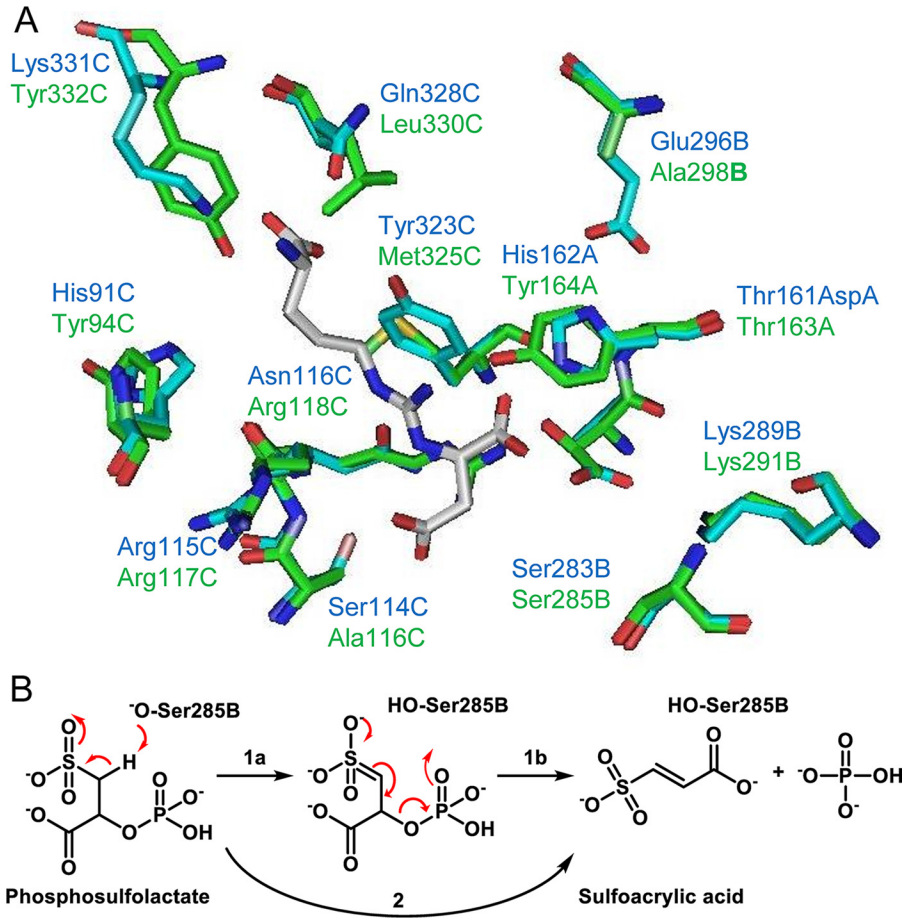


**Figure 5.** *A*, the active site of a canonical δ2-crystallin from duck with bound argininosuccinate (PDB code 1TJW, 76% coverage with 28% ID) with a superimposed homology model for XcbC1 (*cyan* and *green*, respectively). Side chains from each respective chain are denoted with *A*, *B*, or *C*. *B*, the proposed XcbC1 mechanism via an argininosuccinate lyase–type reaction through a general base proton abstraction followed by elimination of the phosphate leaving group. The reaction might occur stepwise (*1*) or in a concerted fashion (*2*).

shaking (180 rpm) in Erlenmeyer flasks sealed with rubber septum stoppers (70, 71). The cells in liquid medium were sparged with compressed air for ~15 min, and propene gas was injected into the headspace (10% volume) every 12 h. The cultures were allowed to reach an optical density at 600 nm ($A_{600}$) of ~1–1.5 before harvesting by centrifugation at 6000 × *g* for 10 min. Aliquots of 5–10 ml were reserved for genomic DNA extraction using the DNeasy blood and tissue protocol for Gram-negative bacteria.

### *Amplification of genes for putative CoM biosynthesis*

Sequences for the putative biosynthetic operon were obtained from the NCBI database file for the pXAUT01 megaplasmid. Primers (Integrated DNA Technologies, San Diego, CA) were designed for *xcbB1* (XAUT_RS24680), *xcbC1* (XAUT_RS24685), and *xcbE1* (XAUT_RS24695) using the respective locus tags given in parentheses (Table S1). Restriction sites were added to clone each gene with an added N-terminal His tag into a Duet expression system (Novagen). The forward and reverse restriction sites for each ORF were as follows: XcbB1, Sac1/Nde1; XcbC1, BamHI/BglII; XcbE1, PstI/EcoRV. Each amplicon was initially cloned into a pGEM-T vector and transformed into JM109-competent cells for propagation before being cloned into a Duet vector. XcbB1 and XcbE1 were inserted into multiple cloning site 1 (MCS1) of individual pETDuet-1 ($Amp^R$) vectors, whereas XcbC1 was cloned under MCS1 of pACYCDuet-1 ($Cm^R$). Sequences were verified via Davis Sequencing (Davis, CA).

### *Expression and purification of putative CoM biosynthesis gene products*

BL21(DE3)-competent cells were transformed with each construct, XcbB1-pETDuet-1, XcbC1-pACYCDuet-1, and XcbE1-pETDuet-1, and cells were grown on lysogeny broth agar plates supplemented with ampicillin (Amp) (0.1 mg/ml) or chloramphenicol (Cm) (0.034 mg/ml), as specified for each construct. A single colony was used to inoculate an overnight culture in liquid lysogeny broth +Amp or Cm medium. Expression was initiated with a 10% volume of the overnight culture (XcbE1 expression included 40 μM pyridoxine) and incubated at 37 °C with shaking at 250 rpm until the culture reached an $A_{600}$ of 0.6–0.8. Protein expression was induced with 1 mM isopropyl 1-thio-β-D-galactopyranoside, and the cells were moved to a 30 °C incubator with shaking at 180 rpm. Protein expression proceeded for 3 h before the cells were harvested by centrifugation (7500 × *g*, 10 min), followed by flash-freezing of the pellets in liquid nitrogen.

For purification, frozen cell pellets were resuspended in lysis buffer (20 mM Tris, 500 mM NaCl, 5 mM imidazole (pH 8)) and homogenized with the addition of lysozyme, DNase, and phenylmethylsulfonyl fluoride. Cell pellets from cultures larger than 1 liter were lysed using a microfluidizer (M-110L Microfluidics Corp., Newton, MA). Lysates were cleared by centrifugation: 45,000 × *g* for 30 min when using a gravity flow column or 105,000 × *g* for 1 h prior to FPLC (Bio-Rad). The nickel-nitrilotriacetic acid columns were equilibrated to the lysis buffer prior to loading the cleared lysate. For FPLC elution, a 75-ml gradient from 0–100% elution buffer was used. The elution buffer contained 20 mM Tris, 500 mM NaCl, 300 mM imidazole, and 20% glycerol. SDS-PAGE and Western blot anti-His tag antibodies (alkaline phosphatase–conjugated monoclonal immunoglobulin from hybridoma clone His-1, Sigma, catalog no. A5588, lot no. 096M4841V) were used to determine the purity of the protein as well as the integrity of the His tag. Buffer exchange of the pure protein into imidazole-free pH 8 buffer (20 mM Tris, 100 mM NaCl) was carried out via centrifuge filtration as a final step prior to storage at −80 °C in 10% glycerol.

### Determining sulfite uptake by the XcbB1-catalyzed reaction

An assay using a fluorescent sulfite indicator was adapted from prior methods (23). Reaction mixtures contained 100 mM Tris (pH 8), 100 mM NaCl, 5 mM $MgCl_2$, 1 mM $NaHSO_3$, and 1 mM PEP in 50 μl. The assay mixture was incubated at 30 °C for 5 min before addition of 0.1 mg XcbB1 enzyme in 50 mM Tris, 50 mM NaCl, and 20% glycerol (pH 8). The reaction was incubated at 30 °C for a further 5 min prior to addition of 5 μl of terminating solution (0.5 M arginine, 0.1 M EDTA adjusted to pH 12.8 with NaOH). Post-termination, 3 μl of 50 mM mBBr dissolved in acetonitrile was added to the assay. The reaction was then incubated in the dark for 15 min at room temperature and diluted to 1 ml using 50 mM glycine and 10 mM EDTA (pH 10). Fluorescence of the sulfite–mBBr adducts was measured on a Cary Eclipse fluorescence spectrophotometer: excitation wavelength 410 nm, emission 480 nm, 350 V photomultiplier tube. Standard curves were generated using a gradient from 0–1 mM $NaHSO_3$ in the reaction buffers. Data fit to linear equations (Kaleidagraph) were used to calculate concentrations of sulfite in enzymatic reactions.

### Measuring inorganic phosphate production by the XcbC1-catalyzed reaction

Phosphosulfolactate produced by XcbB1 was used as the substrate for XcbC1 in a coupled reaction, and the resulting inorganic phosphate was quantified. Samples containing 50 mM Tris (pH 8), 50 mM NaCl, 5 mM $MgCl_2$, 0.1 mg XcbB1 enzyme, 1 mM sulfite, 1 mM PEP, and distilled $H_2O$ in a final volume of 500 μl were incubated at 30 °C for 30 min, followed by incubation at 95 °C for 10 min to stop XcbB1 activity. The samples were centrifuged for 10 min at 14,000 × *g*, and the supernatant was used for the subsequent reaction. To the supernatant, 0.1 mg XcbC1 was added to begin consumption of phosphosulfolactate. The reaction was allowed to continue for an additional 30 min before termination as with XcbB1. The supernatant was then used for phosphate determination.

Formation of inorganic orthophosphate can be detected using ammonium molybdate to form colored molybdenum blue complexes (25, 72). A procedure was adapted from prior methods (73, 74). Briefly, to a 500 μl sample, 100 μl of 2.5 M $H_2SO_4$ was added, followed by 100 μl of 2.5% ammonium molybdate. 10 μl of reducing solution (0.2 g of 1-amino-2-naphthol-4-sulfonic acid, 1.2 g of sodium bisulfite, and 1.2 g of sodium sulfite in 100 ml) was added, followed by distilled $H_2O$ to bring the volume to 1 ml. The samples were thoroughly mixed and then incubated at 50 °C for 15 min. Absorbance was monitored at 700 nm using a Thermo Spectronic Biomate 3. Concentrations of phosphate were calculated from a standard curve generated using $KH_2PO_4$ (0–1 mM).

### Determination of XcbE1 activity with an assay for $H_2S$ formation

The production of $H_2S$ can be detected using a method that converts $H_2S$ to methylene blue with the addition of *N*′,*N*′-dimethyl-*p*-phenylenediamine dihydrochloride (20 mM) in 7.2 M HCl and 30 mM $FeCl_3$ in 1.2 M HCl (75). Enzymatic assays were conducted in sealed crimp vials containing 250 μl of reaction buffer (50 mM Tris and 50 mM NaCl (pH 8)), 0.1 mg of XcbE1, and distilled $H_2O$ to 450 μl. 50 μl of 10 mM L-cys, D-cys, or L-Ala was injected through the septum to initiate the reaction. Reactions were incubated for 1 h at 30 °C, followed by quenching and derivatization with 100 μl each of *N*′,*N*′-dimethyl-*p*-phenylenediamine dihydrochloride and acidified $FeCl_3$. Color development proceeded for 30 min at room temperature. Absorption was measured at 670 nm and referenced to an $Na_2S$ standard (0–150 μM) generated under identical conditions.

### Mass spectrometric analysis of reaction products

Sample buffers were prepared at 1 mM Tris and 1 mM $MgCl_2$ (pH 8) to avoid ion suppression. XcbB1 (0.1 mg) was incubated with 5 mM PEP and 5 mM sulfite for 45 min at 30 °C prior to molecular weight cutoff filtration to remove enzyme. To determine whether phosphosulfolactate was consumed by XcbC1, 0.1 mg XcbC1 was added to the quenched XcbB1 reactions and allowed to react for 20 or 45 min. Samples were quenched by molecular weight cutoff filtration and analyzed by Q-TOF MS without additional derivatization or extractions.

### Q-TOF MS

Analytes were detected with a 6530 series Q-TOF MS equipped with an electrospray ionization source (operated in negative polarity mode), and data were analyzed with MassHunter workstation software version B.03.01 (Agilent Technologies). Samples were introduced via direct injection.

### Time-resolved $^1$H NMR spectroscopy

Time-resolved $^1$H NMR experiments were performed using a 600-MHz ($^1$H Larmor Frequency) Bruker AVANCE III solution NMR spectrometer equipped with a helium-cooled $^1$H-optimized inverse detection ($^1$H, $^{15}$N, $^{13}$C) TCI cryoprobe (Bruker Corp., Billerica, MA). Samples were prepared by first diluting 0.1 mg of XcbB1 in 550 μl of buffer (50 mM Tris, 50 mM NaCl, 5 mM $MgCl_2$, and 10% v/v $D_2O$ (pH 8)), followed by an initial scan

to determine baseline peaks. The substrates PEP and bisulfite were then added to the reaction at varying concentrations (minimum 2 mM PEP for ease of detection) and monitored over the course of 30 min with NMR experiments every 2 min. 1D $^{1}$H NMR spectra were acquired using the Bruker supplied noesygppr1d pulse sequence with 32 scans and a spectral width of 12 ppm, and data were collected into 32,000 data points. Spectral processing and analysis were performed using the Topspin™ software. Approximately 0.1 mg of XcbC1 was added to the reaction upon completion of the XcbB1 time course. The reaction was again monitored over 30 min with scans every 2 min as above.

### *Phylogeny and homology modeling*

27 diverse members of the AFS, including six argininosuccinate lyase family members, were used to construct the maximum likelihood tree on MEGA 6.06 with 100 bootstrap replications. The resulting tree was prepared for publication using FigTree v1.4.2. Homology models for XcbC1 were constructed with SWISSMODEL, using the crystal structure of T161D variant duck δ2-crystallin with bound argininosuccinate (PDB code 1TJW, 76% query coverage, 28% identity).

*Author contributions*—S. E. P., J. L. D., and J. W. P. conceptualization; S. E. P., F. M., A. E. G., H. A. M., B. P. T., and B. M. L. data curation; S. E. P., F. M., and B. M. L. formal analysis; S. E. P., J. L. D., and J. W. P. writing-original draft; F. M., B. P. T., B. M. L., J. L. D., and J. W. P. writing-review and editing; J. L. D. and J. W. P. supervision; J. L. D. and J. W. P. funding acquisition; J. W. P. resources; J. W. P. investigation; J. W. P. project administration.

*Acknowledgments—Support for the NMR instrument console upgrades and Montana State University's NMR Center has been provided by the National Institutes of Health Shared Instrumentation Grant Program (1S10RR13878 and 1S10RR026659), the National Science Foundation MRI Program (DBI-1532078), the Murdock Charitable Trust, and Montana State University's Vice President for Research Economic Development's office. The Proteomics, Metabolomics, and Mass Spectrometry facility at Montana State University received support from the Murdock Charitable Trust and NIGMS, National Institutes of Health (P20GM103474). We thank Dr. George Gauss for technical support and helpful suggestions. We also thank Garrett Moraski and Dr. Robert White for insightful advice.*

## References


1. Balch, W. E., and Wolfe, R. S. (1976) New approach to the cultivation of methanogenic bacteria: 2-mercaptoethanesulfonic acid (HS-CoM)-dependent growth of *Methanobacterium ruminantium* in a pressurized atmosphere. *Appl. Environ. Microbiol.* **32,** 781–791 Medline
2. Balch, W. E., and Wolfe, R. S. (1979) Specificity and biological distribution of coenzyme M (2-mercaptoethanesulfonic acid). *J. Bacteriol.* **137,** 256–263 Medline
3. McBride, B. C., and Wolfe, R. S. (1971) A new coenzyme of methyl transfer, coenzyme M. *Biochemistry* **10,** 2317–2324 CrossRef Medline
4. Taylor, C. D., McBride, B. C., Wolfe, R. S., and Bryant, M. P. (1974) Coenzyme M, essential for growth of a rumen strain of *Methanobacterium ruminantium*. *J. Bacteriol.* **120,** 974–975 Medline
5. Wolfe, R. S. (1990) in *The Molecular Basis of Bacterial Metabolism* (Hauska, G., and Thauer, R. eds.) pp. 1–12, Springer, Berlin
6. Allen, J. R., Clark, D. D., Krum, J. G., and Ensign, S. A. (1999) A role for coenzyme M (2-mercaptoethanesulfonic acid) in a bacterial pathway of aliphatic epoxide carboxylation. *Proc. Natl. Acad. Sci. U.S.A.* **96,** 8432–8437 CrossRef Medline
7. Coleman, N. V., Mattes, T. E., Gossett, J. M., and Spain, J. C. (2002) Phylogenetic and kinetic diversity of aerobic vinyl chloride-assimilating bacteria from contaminated sites. *Appl. Environ. Microbiol.* **68,** 6162–6171 CrossRef Medline
8. Liu, X., and Mattes, T. E. (2016) Epoxyalkane:coenzyme M transferase gene diversity and distribution in groundwater samples from chlorinated-ethene-contaminated sites. *Appl. Environ. Microbiol.* **82,** 3269–3279 CrossRef Medline
9. Mattes, T. E., Coleman, N. V., Spain, J. C., and Gossett, J. M. (2005) Physiological and molecular genetic analyses of vinyl chloride and ethene biodegradation in *Nocardioides* sp. strain JS614. *Arch. Microbiol.* **183,** 95–106 CrossRef Medline
10. Small, F. J., Tilley, J. K., and Ensign, S. A. (1995) Characterization of a new pathway for epichlorohydrin degradation by whole cells of *Xanthobacter* strain py2. *Appl. Environ. Microbiol.* **61,** 1507–1513 Medline
11. van Ginkel, C. G., Welten, H. G., and de Bont, J. A. (1987) Oxidation of gaseous and volatile hydrocarbons by selected alkene-utilizing bacteria. *Appl. Environ. Microbiol.* **53,** 2903–2907 Medline
12. Ensign, S. A., Hyman, M. R., and Arp, D. J. (1992) Cometabolic degradation of chlorinated alkenes by alkene monooxygenase in a propylene-grown *Xanthobacter* strain. *Appl. Environ. Microbiol.* **58,** 3038–3046 Medline
13. Small, F. J., and Ensign, S. A. (1997) Alkene monooxygenase from *Xanthobacter* strain Py2: purification and characterization of a four-component system central to the bacterial metabolism of aliphatic alkenes. *J. Biol. Chem.* **272,** 24913–24920 CrossRef Medline
14. Krum, J. G., and Ensign, S. A. (2000) Heterologous expression of bacterial epoxyalkane:coenzyme M transferase and inducible coenzyme M biosynthesis in *Xanthobacter* strain Py2 and *Rhodococcus rhodochrous* B276. *J. Bacteriol.* **182,** 2629–2634 CrossRef Medline
15. Krum, J. G., Ellsworth, H., Sargeant, R. R., Rich, G., and Ensign, S. A. (2002) Kinetic and microcalorimetric analysis of substrate and cofactor interactions in epoxyalkane:CoM transferase, a zinc-dependent epoxidase. *Biochemistry* **41,** 5005–5014 CrossRef Medline
16. Krishnakumar, A. M., Sliwa, D., Endrizzi, J. A., Boyd, E. S., Ensign, S. A., and Peters, J. W. (2008) Getting a handle on the role of coenzyme M in alkene metabolism. *Microbiol. Mol. Biol. Rev.* **72,** 445–456 CrossRef Medline
17. Ensign, S. A. (2001) Microbial metabolism of aliphatic alkenes. *Biochemistry* **40,** 5845–5853 CrossRef Medline
18. Allen, J. R., and Ensign, S. A. (1999) Two short-chain dehydrogenases confer stereoselectivity for enantiomers of epoxypropane in the multiprotein epoxide carboxylating systems of *Xanthobacter* strain Py2 and *Nocardia corallina* B276. *Biochemistry* **38,** 247–256 CrossRef Medline
19. Clark, D. D., Allen, J. R., and Ensign, S. A. (2000) Characterization of five catalytic activities associated with the NADPH:2-ketopropyl-coenzyme M [2-(2-ketopropylthio)ethanesulfonate] oxidoreductase/carboxylase of the *Xanthobacter* strain Py2 epoxide carboxylase system. *Biochemistry* **39,** 1294–1304 CrossRef Medline
20. Westphal, A. H., Swaving, J., Jacobs, L., and De Kok, A. (2013) Purification and characterization of a flavoprotein involved in the degradation of epoxyalkanes by *Xanthobacter* Py2. *Eur. J. Biochem.* **257,** 160–168 Medline
21. Kofoed, M. A., Wampler, D. A., Pandey, A. S., Peters, J. W., and Ensign, S. A. (2011) Roles of the redox-active disulfide and histidine residues forming a catalytic dyad in reactions catalyzed by 2-ketopropyl coenzyme M oxidoreductase/carboxylase. *J. Bacteriol.* **193,** 4904–4913 CrossRef Medline
22. Pandey, A. S., Mulder, D. W., Ensign, S. A., and Peters, J. W. (2011) Structural basis for carbon dioxide binding by 2-ketopropyl coenzyme M oxidoreductase/carboxylase. *FEBS Lett.* **585,** 459–464 CrossRef Medline
23. Graham, D. E., Xu, H., and White, R. H. (2002) Identification of coenzyme M biosynthetic phosphosulfolactate synthase: a new family of sulfonate-biosynthesizing enzymes. *J. Biol. Chem.* **277,** 13421–13429 CrossRef Medline
24. Wise, E. L., Graham, D. E., White, R. H., and Rayment, I. (2003) The structural determination of phosphosulfolactate synthase from *Methanococcus jannaschii* at 1.7-A resolution: an enolase that is not an enolase. *J. Biol. Chem.* **278,** 45858–45863 CrossRef Medline

25. Graham, D. E., Graupner, M., Xu, H., and White, R. H. (2001) Identification of coenzyme M biosynthetic 2-phosphosulfolactate phosphatase: a member of a new class of $Mg^{2+}$-dependent acid phosphatases. *Eur. J. Biochem.* **268,** 5176–5188 CrossRef Medline
26. White, R. H. (1985) Biosynthesis of coenzyme M (2-mercaptoethanesulfonic acid). *Biochemistry* **24,** 6487–6493 CrossRef
27. White, R. H. (1986) Intermediates in the biosynthesis of coenzyme M (2-mercaptoethanesulfonic acid). *Biochemistry* **25,** 5304–5308 CrossRef
28. Graupner, M., Xu, H., and White, R. H. (2000) Identification of an archaeal 2-hydroxy acid dehydrogenase catalyzing reactions involved in coenzyme biosynthesis in methanoarchaea. *J. Bacteriol.* **182,** 3688–3692 CrossRef Medline
29. Graupner, M., Xu, H., and White, R. H. (2000) Identification of the gene encoding sulfopyruvate decarboxylase, an enzyme involved in biosynthesis of coenzyme M. *J. Bacteriol.* **182,** 4862–4867 CrossRef Medline
30. White, R. H. (1988) Characterization of the enzymic conversion of sulfoacetaldehyde and L-cysteine into coenzyme M (2-mercaptoethanesulfonic acid). *Biochemistry* **27,** 7458–7462 CrossRef
31. Graham, D. E., Taylor, S. M., Wolf, R. Z., and Namboori, S. C. (2009) Convergent evolution of coenzyme M biosynthesis in the Methanosarcinales: cysteate synthase evolved from an ancestral threonine synthase. *Biochem. J.* **424,** 467–478 CrossRef Medline
32. Broberg, C. A., and Clark, D. D. (2010) Shotgun proteomics of *Xanthobacter autotrophicus* Py2 reveals proteins specific to growth on propylene. *Arch. Microbiol.* **192,** 945–957 CrossRef Medline
33. Krum, J. G., and Ensign, S. A. (2001) Evidence that a linear megaplasmid encodes enzymes of aliphatic alkene and epoxide metabolism and coenzyme M (2-mercaptoethanesulfonate) biosynthesis in *Xanthobacter* strain Py2. *J. Bacteriol.* **183,** 2172–2177 CrossRef Medline
34. Puthan Veetil, V., Fibriansah, G., Raj, H., Thunnissen, A. M., and Poelarends, G. J. (2012) Aspartase/fumarase superfamily: a common catalytic strategy involving general base-catalyzed formation of a highly stabilized aci-carboxylate intermediate. *Biochemistry* **51,** 4237–4243 CrossRef Medline
35. Bhaumik, P., Koski, M. K., Bergmann, U., and Wierenga, R. K. (2004) Structure determination and refinement at 2.44 A resolution of argininosuccinate lyase from *Escherichia coli*. *Acta Crystallogr. D Biol. Crystallogr.* **60,** 1964–1970 CrossRef Medline
36. Farrell, K., and Overton, S. (1987) Characterization of argininosuccinate lyase (EC 4.3.2.1) from *Chlamydomonas reinhardtii*. *Biochem. J.* **242,** 261–266 CrossRef Medline
37. Garrard, L. J., Bui, Q. T., Nygaard, R., and Raushel, F. M. (1985) Acid-base catalysis in the argininosuccinate lyase reaction. *J. Biol. Chem.* **260,** 5548–5553 Medline
38. Patejunas, G., Barbosa, P., Lacombe, M., and O'Brien, W. E. (1995) Exploring the role of histidines in the catalytic activity of duck delta-crystallins using site-directed mutagenesis. *Exp. Eye. Res.* **61,** 151–154 CrossRef Medline
39. Paul, A., Mishra, A., Surolia, A., and Vijayan, M. (2013) Cloning, expression, purification, crystallization and preliminary X-ray studies of argininosuccinate lyase (Rv1659) from *Mycobacterium tuberculosis*. *Acta Crystallogr. Sect. F Struct. Biol. Cryst. Commun.* **69,** 1422–1424 CrossRef Medline
40. Sampaleanu, L. M., Codding, P. W., Lobsanov, Y. D., Tsai, M., Smith, G. D., Horvatin, C., and Howell, P. L. (2004) Structural studies of duck delta2 crystallin mutants provide insight into the role of Thr161 and the 280s loop in catalysis. *Biochem. J.* **384,** 437–447 CrossRef Medline
41. Tsai, M., Koo, J., Yip, P., Colman, R. F., Segall, M. L., and Howell, P. L. (2007) Substrate and product complexes of *Escherichia coli* adenylosuccinate lyase provide new insights into the enzymatic mechanism. *J. Mol. Biol.* **370,** 541–554 CrossRef Medline
42. Viola, R. E. (2000) L-aspartase: new tricks from an old enzyme. *Adv. Enzymol. Relat. Areas Mol. Biol.* **74,** 295–341 Medline
43. Puthan Veetil, V., Raj, H., Quax, W. J., Janssen, D. B., and Poelarends, G. J. (2009) Site-directed mutagenesis, kinetic and inhibition studies of aspartate ammonia lyase from *Bacillus* sp. YM55–1. *FEBS J.* **276,** 2994–3007 CrossRef Medline
44. Woods, S. A., Schwartzbach, S. D., and Guest, J. R. (1988) Two biochemically distinct classes of fumarase in *Escherichia coli*. *Biochim. Biophys. Acta* **954,** 14–26 CrossRef Medline
45. Yoon, M. Y., Thayer-Cook, K. A., Berdis, A. J., Karsten, W. E., Schnackerz, K. D., and Cook, P. F. (1995) Acid-base chemical mechanism of aspartase from *Hafnia alvei*. *Arch. Biochem. Biophys.* **320,** 115–122 CrossRef Medline
46. Banerjee, S., Agrawal, M. J., Mishra, D., Sharan, S., Balaram, H., Savithri, H. S., and Murthy, M. R. (2014) Structural and kinetic studies on adenylosuccinate lyase from *Mycobacterium smegmatis* and *Mycobacterium tuberculosis* provide new insights on the catalytic residues of the enzyme. *FEBS J.* **281,** 1642–1658 CrossRef Medline
47. Brosius, J. L., and Colman, R. F. (2002) Three subunits contribute amino acids to the active site of tetrameric adenylosuccinate lyase: Lys268 and Glu275 are required. *Biochemistry* **41,** 2217–2226 CrossRef Medline
48. Bulusu, V., Srinivasan, B., Bopanna, M. P., and Balaram, H. (2009) Elucidation of the substrate specificity, kinetic and catalytic mechanism of adenylosuccinate lyase from *Plasmodium falciparum*. *Biochim. Biophys. Acta* **1794,** 642–654 CrossRef Medline
49. Fyfe, P. K., Dawson, A., Hutchison, M. T., Cameron, S., and Hunter, W. N. (2010) Structure of *Staphylococcus aureus* adenylosuccinate lyase (PurB) and assessment of its potential as a target for structure-based inhibitor discovery. *Acta Crystallogr. D Biol. Crystallogr.* **66,** 881–888 CrossRef Medline
50. Kozlov, G., Nguyen, L., Pearsall, J., and Gehring, K. (2009) The structure of phosphate-bound *Escherichia coli* adenylosuccinate lyase identifies His171 as a catalytic acid. *Acta Crystallogr. Sect. F Struct. Biol. Cryst. Commun.* **65,** 857–861 CrossRef Medline
51. Lee, T. T., Worby, C., Bao, Z. Q., Dixon, J. E., and Colman, R. F. (1999) His68 and His141 are critical contributors to the intersubunit catalytic site of adenylosuccinate lyase of *Bacillus subtilis*. *Biochemistry* **38,** 22–32 Medline
52. Toth, E. A., and Yeates, T. O. (2000) The structure of adenylosuccinate lyase, an enzyme with dual activity in the de novo purine biosynthetic pathway. *Structure* **8,** 163–174 CrossRef Medline
53. Yang, J., Wang, Y., Woolridge, E. M., Arora, V., Petsko, G. A., Kozarich, J. W., and Ringe, D. (2004) Crystal structure of 3-carboxy-cis,cis-muconate lactonizing enzyme from *Pseudomonas putida*, a fumarase class II type cycloisomerase: enzyme evolution in parallel pathways. *Biochemistry* **43,** 10424–10434 CrossRef Medline
54. Soutourina, J., Blanquet, S., and Plateau, P. (2001) Role of D-cysteine desulfhydrase in the adaptation of *Escherichia coli* to D-cysteine. *J. Biol. Chem.* **276,** 40864–40872 CrossRef Medline
55. Eliot, A. C., and Kirsch, J. F. (2004) Pyridoxal phosphate enzymes: mechanistic, structural, and evolutionary considerations. *Annu. Rev. Biochem.* **73,** 383–415 CrossRef Medline
56. Toney, M. D. (2005) Reaction specificity in pyridoxal phosphate enzymes. *Arch. Biochem. Biophys.* **433,** 279–287 CrossRef Medline
57. Watanabe, Y., and Shimura, K. (1956) Biosynthesis of threonine from homoserine: nature of an intermediary product. *J. Biochem.* **43,** 283–294 CrossRef
58. Keller, J. W., Baurick, K. B., Rutt, G. C., O'Malley, M. V., Sonafrank, N. L., Reynolds, R. A., Ebbesson, L. O., and Vajdos, F. F. (1990) *Pseudomonas cepacia* 2,2-dialkylglycine decarboxylase: sequence and expression in *Escherichia coli* of structural and repressor genes. *J. Biol. Chem.* **265,** 5531–5539 Medline
59. Bull, H., Murray, P. G., Thomas, D., Fraser, A. M., and Nelson, P. N. (2002) Acid phosphatases. *Mol. Pathol.* **55,** 65–72 CrossRef Medline
60. Kim, E. E., and Wyckoff, H. W. (1991) Reaction mechanism of alkaline phosphatase based on crystal structures: two-metal ion catalysis. *J. Mol. Biol.* **218,** 449–464 CrossRef Medline
61. Millán, J. L. (2006) Alkaline Phosphatases: Structure, substrate specificity and functional relatedness to other members of a large superfamily of enzymes. *Purinergic Signal.* **2,** 335–341 CrossRef Medline
62. Sharma, U., Pal, D., and Prasad, R. (2014) Alkaline phosphatase: an overview. *Indian J. Clin. Biochem.* **29,** 269–278 CrossRef Medline
63. Simopoulos, T. T., and Jencks, W. P. (1994) Alkaline phosphatase is an almost perfect enzyme. *Biochemistry* **33,** 10375–10380 CrossRef Medline
64. Stec, B., Holtz, K. M., and Kantrowitz, E. R. (2000) A revised mechanism for the alkaline phosphatase reaction involving three metal ions1. *J. Mol. Biol.* **299,** 1303–1311 CrossRef Medline
65. Tabaldi, L. A., Ruppenthal, R., Cargnelutti, D., Morsch, V. M., Pereira, L. B., and Schetinger, M. R. C. (2007) Effects of metal elements on acid

phosphatase activity in cucumber (*Cucumis sativus* L.) seedlings. *Environ. Exp. Bot.* **59,** 43–48 CrossRef
66. Fibriansah, G., Veetil, V. P., Poelarends, G. J., and Thunnissen, A.-M. (2011) structural basis for the catalytic mechanism of aspartate ammonia lyase. *Biochemistry* **50,** 6053–6062 CrossRef Medline
67. Sampaleanu, L. M., Vallée, F., Slingsby, C., and Howell, P. L. (2001) Structural studies of duck δ1 and δ2 crystallin suggest conformational changes occur during catalysis. *Biochemistry* **40,** 2732–2742 CrossRef Medline
68. Zhu, Y., Li, H., Long, C., Hu, L., Xu, H., Liu, L., Chen, S., Wang, D. C., and Shao, F. (2007) Structural Insights into the enzymatic mechanism of the pathogenic MAPK phosphothreonine lyase. *Mol. Cell* **28,** 899–913 CrossRef Medline
69. Ke, Z., Smith, G. K., Zhang, Y., and Guo, H. (2011) Molecular mechanism for eliminylation, a newly discovered post-translational modification. *J. Am. Chem. Soc.* **133,** 11103–11105 CrossRef Medline
70. Wiegant, W. M., and De Bont, J. A. M. (1980) A new route for ethylene glycol metabolism in *Mycobacterium* E44. *J. Gen. Microbiol.* **120,** 325–331
71. Vishniac, W., and Santer, M. (1957) The thiobacilli. *Bacteriol.Rev.* **21,** 195–213 Medline
72. Bessey, O. A., Lowry, O. H., and Brock, M. J. (1946) A method for the rapid determination of alkaline phosphates with five cubic millimeters of serum. *J. Biol. Chem.* **164,** 321–329 Medline
73. Fiske, C. H., and Subbarow, Y. (1925) The colorimetric determination of phosphorous. *J. Biol. Chem.* **66,** 375–400
74. Palmer, R. E. (1985) An experiment to quantitate organically bound phosphate: with special emphasis on biochemical molecules. *J. Chem. Educ.* **62,** 898 CrossRef
75. Todorovic, B., and Glick, B. R. (2008) The interconversion of ACC deaminase and D-cysteine desulfhydrase by directed mutagenesis. *Planta* **229,** 193–205 CrossRef Medline

# Coenzyme M biosynthesis in bacteria involves phosphate elimination by a functionally distinct member of the aspartase/fumarase superfamily

Sarah E. Partovi, Florence Mus, Andrew E. Gutknecht, Hunter A. Martinez, Brian P. Tripet, Bernd Markus Lange, Jennifer L. DuBois and John W. Peters

*J. Biol. Chem. 2018, 293:5236-5246.*
*doi: 10.1074/jbc.RA117.001234 originally published online February 6, 2018*